

CHALMERS



CFD simulation of Flue Gas Flow in Traditional Pottery Furnace

Experimental and Numerical Study of Burning Process and Heat and Mass Transfer Phenomena

Master of Science Thesis

ATIEH KALALI

Department of Chemical and Biological Engineering

Division of Chemical Reaction Engineering

CHALMERS UNIVERSITY OF TECHNOLOGY

Göteborg, Sweden, 2011

CFD Simulation of Flue Gas Flow in Traditional Pottery
Furnace
Experimental and Numerical Study of Burning Process and Heat and Mass Transfer
Phenomena

ATIEH KALALI

Examiner:
Professor Bengt Andersson, Chemical Reaction Engineering, Chalmers University of
Technology

Supervisors:
Dr. Rahman Sudiyo
Professor's assistant Ronnie Andersson

Master of Science Thesis

Department of Chemical and biological engineering
Division of Chemical Reaction Engineering
CHALMERS UNIVERSITY OF TECHNOLOGY
Goteborg, Sweden 2011

CFD Simulation of Flue Gas Flow in Traditional Pottery Furnace
Experimental and Numerical Study of Burning Process and Heat and Mass Transfer
Phenomena
ATIEH KALALI

© ATIEH KALALI, 2011

Department of Chemical and Biological Engineering
Division of Chemical Reaction Engineering
Chalmers University of Technology
412 96 Goteborg, Sweden
Phone + 46 (0)31-772 1000

Cover:
Picture of a traditional ceramic furnace in Pundong, Indonesia.

CFD Simulation of Flue Gas Flow in Traditional Pottery Furnace
Experimental and Numerical Study of Burning Process and Heat and Mass Transfer
Phenomena
ATIEH KALALI
Department of Chemical and Biological Engineering
Division of Chemical Reaction Engineering
Chalmers University of Technology

Abstract

One of the many pleasures of visiting Indonesia is having the opportunity to get to know about country's art and handicraft such as ceramic. A clay body's journey in the traditional pottery industry contains several stages. Process improvements are traditionally based on working experience. The process and quality of the pottery must be improved due to competitiveness. In order to produce high quality pottery better burning process is needed. The purpose of the project is to analyze the burning process in a traditional furnace in order to increase the temperature and decrease the fuel consumption. The process is studied during two months in a village named Pundong in Java with purpose of observing drying process of ceramic bodies in different stages and collecting temperature data to develop a water evaporation model in CFD. These data are used to do CFD simulations of the burning process in a software program named FLUENT. The simulations cover the vaporization of free and bound water in the clay bodies and also a radiation model. The results show that the furnace does not reach the maximum temperature of 900°C and therefore no vitrification process occurs. The temperature is sufficient to remove free water and chemically bounded water. The CFD results show that the difference of the temperature between the area close by wall and the bulk flow is huge. It also shows that the densely packing of the clay bodies inside the oven is a source of error.

Keywords: ceramic furnace, CFD, natural convection, bound water, evaporation of water, radiation

Acknowledgment

I am enormously thankful to my examiner Professor Bengt Andersson whose encouragement, guidance and support from the initial to the final level enabled me to develop an understanding of this thesis.

Thanks to Dr. Rahman Sudiyo; my supervisor in University of Gadjah Mada (UGM), Indonesia.

Thanks to Professor's assistant Ronnie Andersson for his help.

Thanks to PhD student Per Abrahamsson for his constantly and kindly support.

I would like to thank all the staff and students at the Chemical Engineering department in UGM and also in Chalmers, for pleasant and helpful atmosphere.

Finally I would like to appreciate my family for all their love and nonstop support.

Table of Contents

- 1. Introduction..... 10
 - 1.1 Aim 10
 - 1.2 Thesis Outline 10
- 2. Background..... 10
 - 2.1 New Design of Traditional Furnaces 10
 - 2.2 Preparation of Green Body 12
 - 2.3 The Burning Process in Practical Steps 13
 - 2.3.1 Packing..... 13
 - 2.3.2 Burning 15
 - 2.3.3 Ending the Burning 16
- 3. Theory 17
 - 3.1 The Structure of Clay (An Introduction to Ceramic Material) 17
 - 3.1.1 The Nature of Clay and Clay-Water Relationship 18
 - 3.2 Drying Process of the Clay Bodies 18
 - 3.2.1 Firing..... 20
 - 3.2.3 Equilibrium Moisture 21
 - 3.3 Heat Transfer 21
 - 3.3.1 Conduction..... 21
 - 3.3.2 Convection 21
 - 3.3.3 Natural Convection 22
 - 3.3.4 Radiation 22
 - 3.4 CFD Theory 23
 - 3.4.1 Single Phase Flow..... 23
 - 3.4.2 Modeling of Turbulent Flow..... 23

3. 4.3 Transport Equations	23
3.4.4 Turbulence Models - Two Equation Models	24
3.4.5 k- ω Models.....	25
3.4.6 Reaction Modeling.....	25
3.4.7 User Defined Function (UDF)	26
4. Method	26
4.1 Measurement of Temperature Data.....	26
4.1.1. Limitation of Work	26
4.1.2. Weight Measurement of Clay Body.....	26
4.2 Heat Phenomena	26
4.2.1 The Method behind Natural Convection.....	27
4.2.2 Assumption	28
4.2.3 Calculation of Heat	28
4.3 CFD.....	29
4.3.1 Geometry.....	29
4.3.2 Mesh.....	30
4.3.3 Setting in FLUENT and Assumption.....	31
4.3.4 Boundary Condition.....	31
4.3.5 Develop a Method for Evaporation and Langmuir Isotherm	32
4.3.6 Assumption in Evaporation Model	33
4.3.7 Bound Water and Evaporation.....	33
4.3.8 Radiation Model.....	34
5. Result and Discussion	35
5.1 Experimental Results	35
5.1.1 First Experience (Coal & Wood)	35
5.1.2 Second Experience (Firewood).....	37

5.2 Discussion of the Experimental Results.....	39
5.3 CFD Results	40
5.4 Discussion of the CFD Results	47
6. Conclusions.....	48
7. Future Work.....	49
8. References.....	50
Appendix A.....	51
Appendix B.....	52
Appendix C.....	54
Appendix D.....	56

1. Introduction

One of the many pleasures of visiting Indonesia is having the opportunity to get to know about country's art and handicraft such as ceramic. Ceramic has been found its way to Indonesia over centuries of trade with China. There is a wide range of items from everyday household pieces such as vases, pots and plates, to creative ceramic objects such as Buddha statues. Some types of ceramic pottery made in villages near Yogyakarta, Java are loved by many people.

The pottery industry is one of the most important sources of economic income for many families in Java. For many generations, this industry has been continued based on working experiences which make it weak and insignificant. To heighten the level of knowledge in the rural areas a lot of efforts have been done by the University of Gadjadja (UGM), Yogyakarta to make a bridge between the rural people and the academics. This would help all the traditional industries to include the pottery industry and to produce the products which are capable to compete with the similar ones in the world market.

Some cooperation between Chalmers University of Technology and UGM in form of research and study has been done to achieve progress in this traditional pottery industry. The presented project is just one of the links in the chain. In order to improve the quality of the products and decreasing the cost of the production it is needed to optimize the burning process in traditional furnaces.

1.1 Aim

The purpose of the project is to analyze the burning process in a traditional furnace in order to find a method to be able to explain water evaporation in the porous of clay and also study the effect of radiation in drying process. As an approach, the drying process of ceramic bodies in several stages has been observed, and finally a developed water evaporation model has been introduced in this thesis.

2. Background

2.1 New Design of Traditional Furnaces

In Java the fuel of the burning process in furnaces is usually firewood whose availability has been decreasing and its price has been increasing during past years. The quality of the pottery depends significantly on both the quality of the clay and the burning process. Thus it is important to evaluate whether the heat value of firewood is sufficient enough to obtain adequate temperatures in the furnace or not. After some experiences, the idea of either changing the fuel or mix it up with another one has been introduced.

Coal briquette can be a good option as the fuel in traditional furnaces to increase the temperature inside and some experiences have been done to mix the wood and briquette. The result showed a very good temperature increasing in shorter period without any cracking in the pottery bodies but the problem is that the structure of the very old traditional kilns cannot tolerate the high temperatures. Besides, the efficiency is still too low due to the poor design of these kinds of furnaces.

Therefore a new design and a new type of traditional kiln seems to be required since raising the temperature until sufficient level helps to gain better quality at the bodies. It also gives possibility to design new and modern shapes of bodies in order to compete with Chinese models.

The idea of designing a new traditional furnace becomes operational after the University of Gadjara Mada has been paid by the Ministry of Science in Indonesia. The work has been started by searching in literature. The task is finding a proper and cheap design which can increase the efficiency largely. In the village Pundong there is such a kiln by a design close to the literature ones. It is told that the modern furnace is a copy from the Chinese's one and it can increase the quality of the potteries. That furnace had not been used for a long time due to its small size.

The furnace in the first visit is shown in Figures 1 and 2.



Figure 1: a picture of Pundong traditional furnace. To the left, the furnace together with the exhaust tower, and to the right, close up from the kiln.



Figure 2: The furnace from the side. To the left, the furnace with the fire placement, and to the right, close up from the fireplace.

As figures 1 and 2 confirm, the oven is dirty and completely not used for a long time. As can be seen, Figure 1, to the left shows the overview of the whole furnace includes the tower for exhaust gas. The distance between the tower and the body of kiln is 121 cm. Figure 1, to the right is a close up from the front side of the furnace. Figure 2 shows the picture taken from the left side of the kiln. As seen, the entrance of fire placement with the dimension of 37×54 cm is located at the bottom of the kiln. There is another one in the other side of the kiln with exactly the same size. The depth of these fire placements is the same as the width of the kiln, i.e. the heat flow pass the whole way under the kiln and then goes inside the furnace through the internal holes with the dimensions of 23×39 cm. For dimensions of the furnace see appendix A.

2.2 Preparation of Green Body

The clay is mixed with sand and water. The mixture is then rolled to 2-3 cm thickness and formed by hand into the favorite shape (See figure 3).



Figure 3: Preparation of green body.

A body that is dried and formed but not fired yet is called green body. The green bodies are usually hollow. They are placed outdoors for at least 3-4 days in dry seasons and 4-7 days in wet seasons to allow them become dry. The bodies should be avoided direct sunshine exposure due to preventing fast drying rate.

2.3 The Burning Process in Practical Steps

2.3.1 Packing

The packing process in the kiln has no regulation. The furnace is densely packed with green bodies where the small bodies fill the empty space between the bigger bodies. The size and shape of the bodies depend on the market demand and can be different every batch. The main task during packing the oven is to fit in as much bodies as possible to save time and energy. As can be seen in figure 4, the direction of the open hole of the body depends on the dense packing possibility.



Figure 4: Pcking in the furnace.

As it shown in figure 4, clay bodies have been placed close to each other with no expanse or plate between them. The biggest bodies have been stood in the back part while the middle-sizes are in the bottom and the smallest bodies are above them.

Figure 5 shows the placement of clay bodies close to the entrance of the heat flow inside the oven.



Figure 5: Packing close to the entrance of heat flow.

The entrance of heat flow should be kept open therefore a surrounded wall is made around the holes by some bricks. The two most important effects of building the wall around the holes are: First, It protects the heat flow entrance from being covered by the bodies. Second, the wall around the opening causes the heat flow to go up and then hits the roof and after that comes down which has an effect of making more turbulent heat flow inside the oven. Figure 6 shows how the entrance of the furnace is covered by bricks.



Figure 6: Closing the entrance of the kiln. To the left, the bricks are used and to the right, the small distances are covered by clay soil.

Some bricks in the same material of the bricks, which are used in the structure of the oven, are used to close the front opening. For covering the remained small open parts, the clay soil and also asbestos are used in some parts, however it does not cover all the open spots perfectly.

2.3.2 Burning

In some occasions, the burning process starts by burning some rubber and using diesel oil as it can be seen in figure 7.



Figure 7: burning process starts by burning some rubbers.

Using rubber and oil makes the burning process easier especially when using wet season firewood. At the beginning, the fire should be in the entrance of the fire place in order to get more oxygen from the air. Taking care of the fire in both sides is very important to have a steady fire to gain the steady temperature in the whole kiln.

By starting the fire, the measurement of temperature is started. In this presented work, six points, have been chosen, three in the front and three in the back side of the kiln, to measure the temperatures (See figure 8).



Figure 8: Temperature measurement points. To the left, the points in front of the kiln and to the right, the points in the back side are shown.

The points in the back side of the furnace are named A, B and C. The points in the front side are named D, E and F. The temperature is measured in small time intervals in the beginning due to have a better possibility for studying the effect of convection and preheating period, but after 120 minutes the interval of 60 minutes for each measurement is chosen.

The temperature of exhaust gas is also measured as seen in figure 9.



Figure 9: Temperature measurement of exhaust gasses.

This measurement is done hourly.

2.3.3 Ending the Burning

The fuel feeding is stopped and after that the fire place is closed as it seen in figure 10.



Figure 10: canceling the fire.

The burning process is stopped when the pottery bodies start to “glow”. The entrance of fire placement is blocked due to stop the air reaching the fire. In some cases, the fire is stopped more rapidly.

3. Theory

In this part the theory behind of the process is explained.

3.1 The Structure of Clay (An Introduction to Ceramic Material)

The Clay Minerals are a part of a general group within the Phyllosilicates that contain large percentages of water trapped between their silicate sheets with two structural units, such as silica (SiO_2) and alumina (Al_2O_3). The silica sheet is formed of tetrahedron consisting of Si^{4+} which is surrounded by four oxygen atoms. The oxygen atoms are shared by adjacent tetrahedra. These tetrahedra are repeated to arrange a hexagonal network where the sheet composition is $\text{Si}_2\text{O}_5^{2-}$. The alumina sheets consist of octahedra where Al^{3+} is surrounded by six hydroxyl groups. The clay minerals are formed by the aluminum hydroxide layers that condense with the silica sheets. Water is bounded to the layer structures as hydroxyl groups. The fact that the atoms are not closely packed together results in relatively low density which is an important property of clay material. The strength of bonds results in a high melting temperature.

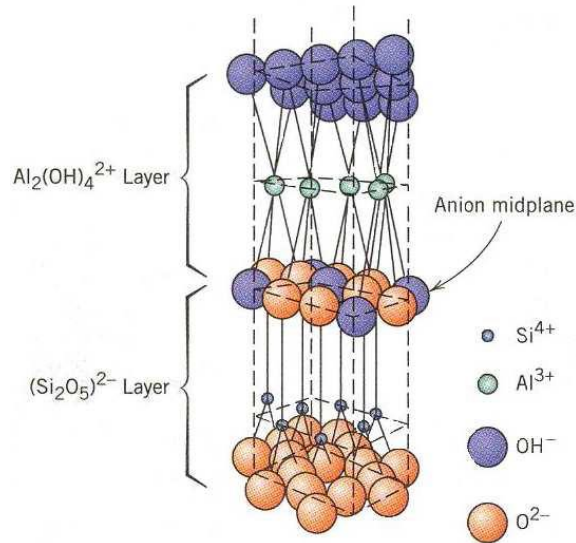


Figure 11: The two-layer structure of kaolinite, showing the hydrogen bonds between the OH groups.

The type of clay that is used in Java is a mixture of kaolinite and halloysite. In this thesis halloysite is assumed to behave the same as kaolinite when it comes to heat properties and water loss. Pure kaolinite is white and pure halloysite is brown. Both these clay types belong to the kaolin group. All kaolin clays consist of the same silicate structure and are chemically the same. The types are unique based on the way the layers are stacked. As shown in figure 11, kaolinite ($\text{Al}_2\text{Si}_2\text{O}_5(\text{OH})_4$) has negative charges on the faces. The crystals consist of two-layer structure where the layers are bounded together with hydrogen bonds between the OH groups [1].

3.1.1 The Nature of Clay and Clay-Water Relationship

Clay usually contains one or more clay minerals as well as accessory minerals, such as iron oxides. Clay used in Pundong includes some iron compounds and the “glowing” effect at the end of burning process is a result of releasing Fe_2O_3 . Clay is a unique group of materials. They differ from the others due to their behavior when associated to the water. During the forming operation, water is added to the clay to get plasticity. The water appears as thin water films which separates the clay particles and makes them free to move over one another. The plasticity is in a compromise with the porosity to form good quality clay. The porosity controls the migration of water during the drying process.

3.2 Drying Process of the Clay Bodies

After forming the clay to the bodies, drying is the next important step. The rate of drying against the water percentage remaining in the piece is plotted in figure 12. It can be observed that the rate of drying is constant during the initial stages and then decrease dramatically.

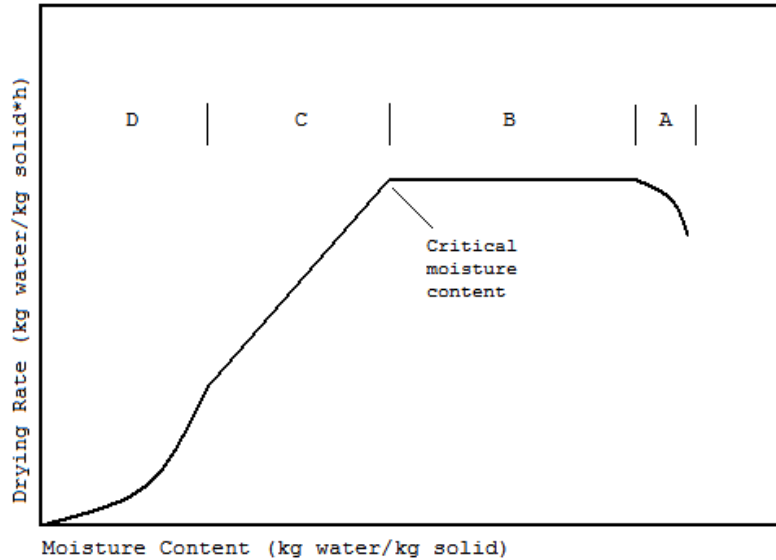


Figure 12: The drying rate versus moisture content.

The first period (A) is called heating period when the dry object is cold and slowly gets warmer by the circulating flow. The constant rate period of drying (B) corresponds to removal of water from the surface. This occurs between approximately 80°C-200°C. As this water is removed the piece starts to shrink hence, a continuous water layer is maintained on the surface. When most of the easily accessible water has been evaporated the process reaches the point named the critical moisture content and it is when period C starts.

The first falling rate period (C) will give almost a constantly decreasing drying rate. This is when the particles come in contact with each other and shrinkage ceases. Continued drying causes the water surface to retreat further beneath the surface of water therefore it is more difficult for the moisture to evaporate and drying rate decreases. Diffusion of the water vapor inside a material is the limiting step in this period, and as the diffusion path increases the rate of drying will decrease linearly. The shrinkage is influenced by the thickness of the body, the water content and the size of the clay particles. The shrinkage factor can be controlled by temperature, humidity and airflow. The temperature distribution must be equal in the oven. If the top of the body is warmer than the bottom, the top will shrink faster which can cause warps or cracks. When outside and inside temperatures of clay body are different there is a risk for one side expanding and one side shrinking.

The last period, if it exists, is a second order process. When most of the water in a clay body is exhausted the drying enters the second falling rate period (D). The rate in this period falls rapidly with moisture content. The period is limited by diffusion of liquid water within a body or grain [2].

The stages of the drying process are shown in figure 13.

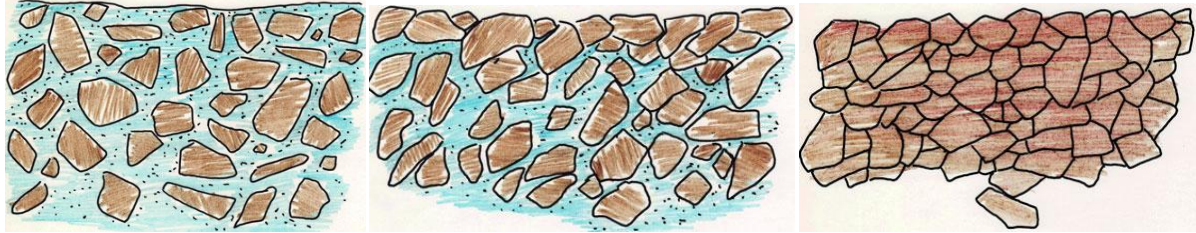


Figure 13: The different stages of the drying process.

During the drying process, the free water is removed from the clay. There is a surface gradient due to diffusion of water from the interior of the clay body to the surface and evaporation of water on the surface. If the evaporation rate is larger than the diffusion rate, the surface will dry and there will be risk for cracks. The size of the pores is determining the diffusion rate. Very fine grained clay must be dried very slowly due to the generated steam cannot migrate through the pores and the pressure cause the cracks [2].

3.2.1 Firing

Chemically bound water cannot be removed by drying. Only at temperature range 450-600°C this water is removed [1]. The firing is a critical procedure of the clay treatment because mostly in this stage the cracks would occur. Sufficient temperature interval for the firing is between 900–1400°C. At 900°C a number of chemical reactions will begin which will improve the clay properties and increase the density. At 980 °C the clay decomposes to alumina and amorphous silica and around 1100°C mullite formation happens. In the traditional pottery industry 900°C is a suitable temperature to reach. At this temperature the body will be strong and dense when the cooling of the clay initializes [1].

3.2.2 Bound & unbound water

A liquid inside a porous material can be unbound or bound. The unbound liquid behaves like free water and is not adsorbed in any way to the material. The bound water is characterized by an adsorption heat, and a lower enthalpy state. To be able to be evaporated, the adsorbed water requires additional heat. This heat of wetting may be approximated (according to Smith and van Ness [2]) by assuming that the vapor phase acts as an ideal gas and that the volume of the condensed phase is negligible compared to that of the vapor phase.

A solid object containing bound water, and in equilibrium with its surroundings, will have a vapor pressure that is lower than the saturation pressure at a set temperature. We define the activity A as the ratio of the vapor pressure of the bound water to the vapor pressure of a free water surface. The value of A depends mainly on the size of the pores in the solid material, which will lower the exerted vapor pressure. Smaller pores will have the effect of more difficult transport and a lower activity.

In reality there are three main types of bound water. Water can be placed in small pores, which will make it more difficult to evaporate since the pores will lower the possible vapor pressure to be exerted by the gas. It can also be adsorbed onto a surface, a state which has an additional enthalpy in the range of 1-10 kJ/mol. Finally, water attached by chemical bonds. This will give an extra enthalpy of >10 kJ/mol.

3.2.3 Equilibrium Moisture

When a wetted object is in equilibrium with the surrounding air, at constant T, P and humidity the moisture left in the object is said to be the equilibrium moisture content. Let basis moisture content as X and define the equilibrium moisture as X^* . The difference between them is called the free moisture X_f . This is the amount of moisture that can be released before the system reaches its equilibrium and is an important term since it can be seen as a driving force for the evaporation [3].

$$(3.1) \quad \text{---} \quad (3.2)$$

According to Keey [3], the dependence of the equilibrium moisture content with temperature can be correlated by the above expression. α is said to vary between 0.005 and 0.01 (1/K).

3.3 Heat Transfer

Heat transfer occurs in three different types which are conduction, convection and radiation. The heat flow inside the furnace is caused by natural convection.

3.3.1 Conduction

Conduction is heat transfer through a solid body from hotter to colder region which is described by Fourier's law, (3.3). Conduction in the furnace would occur through the clay bodies, bottom of the furnace and the walls [4].

$$\text{---} \quad (3.3)$$

Where k is defined as thermal conductivity.

3.3.2 Convection

Convection is heat transfer between solid and fluid which is described by Newton's law of cooling, equation (3.4). The heat transfer between surfaces and flue gas is due to convection. It is assumed to be natural (free) convection due to no fan forces in the system [4].

$$\text{---} \quad (3.4)$$

Where, h is convection coefficient.

3.3.3 Natural Convection

When heat is added to a fluid there will be a fluid motion caused by the heat transfer. This is due to that the fluid density will vary with the temperature. The density change and force of gravity will introduce a natural circulation. This natural circulation is termed natural convection. The flow through the furnace is caused of this natural circulation. There is no fan or other equipment which forces the air flow through the oven. The air flow is heated in the furnace and the density becomes gradually lighter and the air rises. This will cause a pressure difference between the furnace top and bottom which shown in figure 14. The height of the chimney and the temperature gradient affects the pressure difference [4]. The effect is often named as chimney effect. The pressure difference is used in the calculation of the inlet velocity.

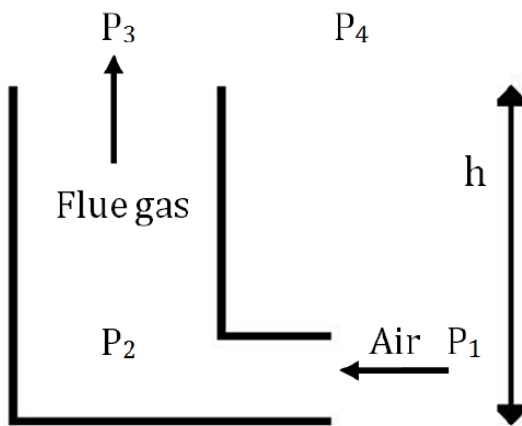


Figure 14: the pressure difference between the top and bottom of the furnace.

Here will be a vertical movement of air at the furnace walls which is caused by a similar effect to the chimney effect because the surfaces are colder than the adjacent air. The density difference will cause cold air fall down the walls and there will be a replacement with new air. This causes a natural circulation called downdraught which is affected by the height of the walls and also the temperature of the walls.

3.3.4 Radiation

Radiation is energy emission from a warm surface to a cold surface. Radiation is represented in equation (3.5). The emitted energy amount is due to both temperature differences between the two surfaces and the level of the temperature. That is why radiation is becoming important at high temperatures. In the furnace, there will be radiation from the clay bodies to each other and to the oven walls and from the walls to the clay bodies [4].

–

(3.5)

Where, ϵ is the emissivity. It is defined as the ratio of the total emissive power of a surface to the total emissive power of an ideally radiating surface at the same temperature. The ideal radiating surface is also called a black body [4].

3.4 CFD Theory

Computational fluid dynamics (CFD) is a tool for solving the Navier Stokes equations (N.S.) numerically by computer software. N.S. are differential equations that describe the motion of a fluid. CFD utilizes N.S. for solving momentum, heat and mass transfer for a certain geometry. The geometry is divided into computation cells, and then N.S. are solved numerically for each cell in an iterative manner. The quality of geometry resolution, input data and software knowledge affects the result significantly. Usually computer capacity is a limiting factor. The results can give a picture of temperature distribution and flow field, but must be analyzed with critical eye. CFD is a step by step method which must be developed to give proper results. An advantage with CFD is that it is possible to get detailed knowledge of a system rather fast. This makes CFD very useful for both existing systems and preliminary studies for the functionality of new systems [5].

3.4.1 Single Phase Flow

In single phase turbulent flow most simulations can be obtained, however some problems in simulation of fast reactions would occur. In present project, the vaporization of water from the clay body surfaces is a fast reaction. When the reaction rate is fast the iterations become unstable and the solution will diverge [5].

3.4.2 Modeling of Turbulent Flow

Turbulence enhances mass transfer and chemical reaction and is often encountered in industrial applications. It is therefore interesting from an engineering point of view to be able to simulate turbulence. Turbulence is a state of the fluid flow, which can be considered as chaotic and random. The most characteristic features of turbulence flows are its irregularity (different shape, size, etc.), diffusivity, instability, three dimensional structures and its dissipation of the kinetic energy. All these characteristics together, make turbulent flows very random and difficult to model. Many models, based on different assumptions, are available and they all have different applicability and limitations. The model used in this project is $k-\omega$ model which is described in 3.4.4 Turbulence Models - Two Equation Models.

3.4.3 Transport Equations

The transport mechanisms for mass, heat, and momentum in turbulent flow are described by the random movement of turbulent eddies. The transportation of species, energy, and momentum is modeled in the turbulence models.

The equation of Continuity is described by:

$$\rho \frac{D\mathbf{u}}{Dt} = -\nabla p + \mu \nabla^2 \mathbf{u} \quad (3.6)$$

For constant density and viscosity and with combination in the momentum equations, the continuity equation forms a more numerically suitable equation, the so called Poisson equation for pressure:

$$\nabla^2 p = -\nabla \cdot \mathbf{u} \quad (3.7)$$

In engineering perspective it is desirable to simplify the equation even more. With the assumption of incompressible flow with constant density along the stream line the continuity equation forms:

$$\nabla \cdot \mathbf{u} = 0 \quad (3.8)$$

The momentum equation is described by the Navier-Stokes equations:

$$\rho \frac{D\mathbf{u}}{Dt} = -\nabla p + \mu \nabla^2 \mathbf{u} \quad (3.9)$$

For a Newtonian fluid the Navier-Stokes equation forms:

$$\rho \frac{D\mathbf{u}}{Dt} = -\nabla p + \mu \nabla^2 \mathbf{u} \quad (3.10)$$

Except for the continuity equation and momentum equations FLUENT also solves the energy and species balance. The heat balance is explained by the addition of the kinetic energy balance and chemical reactions:

$$\rho c_p \frac{DT}{Dt} = \nabla \cdot (\mathbf{u} T) + \nabla \cdot (\mathbf{q}) + \dot{q}''' \quad (3.11)$$

The species balance for constant density fluid is described by:

$$\rho \frac{Dc_i}{Dt} + \nabla \cdot (\mathbf{u} c_i) = \nabla \cdot (\mathbf{D}_i \nabla c_i) + \dot{c}_i''' \quad (3.12)$$

The concentration is in most CFD programs replaced with mass fraction:

$$\rho \frac{Dc_i}{Dt} + \nabla \cdot (\mathbf{u} c_i) = \nabla \cdot (\mathbf{D}_i \nabla c_i) + \dot{c}_i''' \quad (3.13)$$

3.4.4 Turbulence Models - Two Equation Models

For general simulations of turbulence flow the two-equation models are often used due to their robustness and relative inexpensive computational cost. With more equations to solve the computational time increases. However to determine the local turbulence, i.e. the velocity and

length scales, two additional equations for closure of the RANS equations are beneficial. The two-equation models solve the turbulent velocity and length scale independently. The turbulence production and dissipation transportation can have localized rates. One approach to determine the local turbulence is to solve the turbulent kinetic energy (k) equation for the velocity scale and one equation with a property that can determine the length scale. Examples of properties are vorticity scale (ω), time scale (τ), dissipation rate (ε) and of course the length scale (l).

3.4.5 k - ω Models

The length scale determining property in the k - ω model is the specific dissipation, ω . It should be interpreted as the inverse of the dissipation time scale. The modeled k -equation and ω – equation are described by:

$$\frac{dk}{dt} = P_k - \varepsilon_k + \nabla \cdot (D_k \nabla k) \quad (3.14)$$

$$\frac{d\omega}{dt} = P_\omega - \beta \omega^2 + \nabla \cdot (D_\omega \nabla \omega) \quad (3.15)$$

Where α , β , γ , δ , and σ are closure constants. The turbulent viscosity also needs to be determined and is described by:

$$\mu_t = \frac{\rho k}{\omega} \quad (3.16)$$

The k - ω model is a reliable choice for low Reynolds numbers flows when both k and ε approach zero. No wall functions are needed since the k - ω model can predict the law of the wall in the viscous sub-layer. However since a very dense mesh close to the wall is required, first grid below $y^+ = 5$, for the low turbulence k - ω model, wall functions can be used to increase the computational efficiency. Another advantage is that the k - ω model has the ability to predict boundary layers with adverse pressure gradients and separating flows.

3.4.6 Reaction Modeling

In this thesis the laminar finite-rate model computes the reaction rate, where the reaction occurs in the porous body and the flow is laminar. It is an accurate model for laminar systems and it works acceptable for low turbulent flows [6]. The reaction rate is determined by the Arrhenius expression (See equation (3.17)).

$$r = A e^{-E/RT} \quad (3.17)$$

Where, A is pre-exponential factor and E is activation energy [4].

3.4.7 User Defined Function (UDF)

A user defined function is a data file that contains the information, e.g. equations or correlations, FLUENT needs to be able to solve transport equations. The UDF used for the presented project includes equations to explain the radiation. An absorption coefficient has been introduced in FLUENT to vary the bodies which reflect the heat from the ones which absorb it.

4. Method

To cover all implemented parts of the thesis the method chapter is included all practical works done in Indonesia with related heat calculations and also CFD simulations done at Chalmers.

4.1 Measurement of Temperature Data

Two series of temperature measurements were accomplished in Pundong, Indonesia. The difference between series was the fuel. In the first try a mixture of wood and coal briquette is used while in the second one only wood. The data used in CFD simulations are from the second measurement. As stated in chapter 2 the working situation in traditional pottery industry in Java is complex. The market supply and demand of pottery determines the production. Hence, there is no regular schedule for the burning processes and occasions for burning process can be cancelled with short notice, which makes it difficult to plan to do more experiences in a shorter period.

The temperature is measured with a thermocouple on marked point (See figure 8) on the walls both inside and outside of the furnace. The initial temperature is measured before the firing process started, and then measurements are done in small time intervals in the beginning due to have a better possibility for studying the effect of convection and preheating period but after 120 minutes the interval of 60 minutes for each measurement has been chosen.

4.1.1. Limitation of Work

Sometimes during the burning process, one of the fires is completely off and it takes few minutes to be on again. It is important that the fires be controlled regularly and get fed equally. During one of the experiments one of the temperature measurement's points has been blocked by a pottery body only few minutes after burning. The reason is not known. It can depend on that the bodies have rolled on each other in some way.

4.1.2. Weight Measurement of Clay Body

Before and after each burning process all the clay bodies' weight is measured. The difference in weight is the water loss for each clay body which is assumed to be vaporized water.

4.2 Heat Phenomena

There is conduction through the walls which is calculated and calculations are based on the temperature measurement from both inside and outside of the furnace. Data is taken from the north and south sides which are assumed to be more realistic. The west and east walls have a

higher outside temperature but that is probably because of heat losses in warm flue gas from the area where firewood is fed.

The radiation effect is more important when the free water is vaporized and the temperature increases in the furnace. There is not any radiation from flue gas before reaching 900°C, which is not reached in the most cases of burning in traditional pottery furnaces. However there is radiation from the clay surfaces and the kiln's walls inside that may be larger than convective heat transfer when the process has reached the temperature at about 600 °C or 700°C. The problem is that clay body temperature is not known which makes it more difficult to calculate the radiation in heat calculations.

4.2.1 The Method behind Natural Convection

As stated in chapter 3.3.3 the air goes into the furnace through the natural convection. The calculation of the inlet velocity is based on the pressure gradient which is imposed in the furnace. Figure 15 shows how the pressure changes from atmospheric pressure P_1 to P_2 .

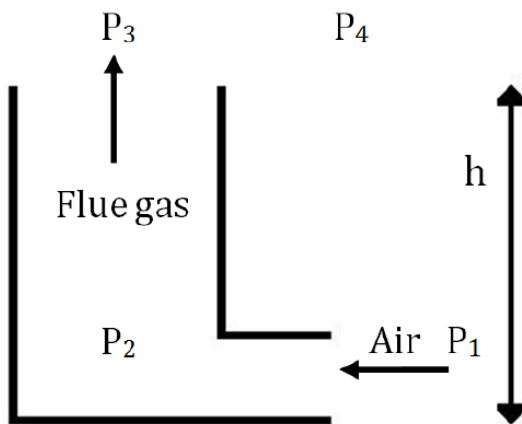


Figure 15: the pressure gradient in the oven.

The calculation is based on equation (4.1) which calculates the hydrostatic pressure.

$$(4.1)$$

To calculate ρ and μ , equations (4.2) and (4.3) are used.

$$(4.2)$$

$$(4.3)$$

Where ρ and μ are equal to

$$(4.4)$$

Equation (4.4) shows the pressure difference in the kiln.

The Bernoulli equation is determined to calculate the inlet velocity based on the pressure gradient. Then equation (4.5) is the Bernoulli equation and the inlet velocity will be calculated by equation (4.6).

$$\frac{1}{\rho} \frac{dp}{dx} = -\frac{dV}{dx}$$

4.2.2 Assumption in Heat Calculation

Heat losses over the all furnace's walls are assumed to be equal. The vaporization of free water is specified taking place when the temperature is 80°C until 200°C. The weight loss of the clay bodies is assumed to be vaporized free water and vaporizing temperature is set to be 100 °C. The radiation is excluded from the calculations.

4.2.3 Calculation of Heat

To be able to calculate the efficiency of the traditional furnaces, the amount of heat loss must be determined. As indicated in chapter 2.1 two burning processes are experimented to collect data for this project. In the first case a combination of wood and coal briquette has been used while in the second one only firewood used as fuel. The shown calculation in this section summarized the second case when fire wood is the only fed fuel. In order to see the complete calculation for both cases see appendix B and C. The given energy to the furnace is based on the total amount of firewood and the wood enthalpy and can be obtained from equation (4.7).

$$(4.7)$$

The heat calculation of consumed energy is based on the water loss of the clay and the sensible heat in gas and solid. The added energy is required to heat the water in clay bodies from initial surrounding temperature to vaporization temperature which assumed to be exactly 100°C (See equation (4.8)).

Later, this energy is used to vaporize the water as shown in equation (4.9).

$$(4.9)$$

The clay mass must be also heated from the initial room temperature to a final temperature as it stated in equation (4.10).

$$)$$
 (4.10)

The heat loss of the burning process, which is through the walls and the top of the kiln and also from the fire placements, can be estimated from equation (4.11).

4.3 CFD

The real furnace packed with a lot of clay bodies is complicated to model. The simulation method in this thesis is a method with a simple geometry and three clay bodies in it. The presented model has a good quality mesh especially close to the walls where the vaporization needs to be studied closely. The first basic set up case has been developed step by step by adding water in the system.

4.3.1 Geometry

Figure 16 shows the final design of the clay bodies inside the oven. The geometry is created in ANSYS Workbench. To reduce the computational time, a simple model is used.

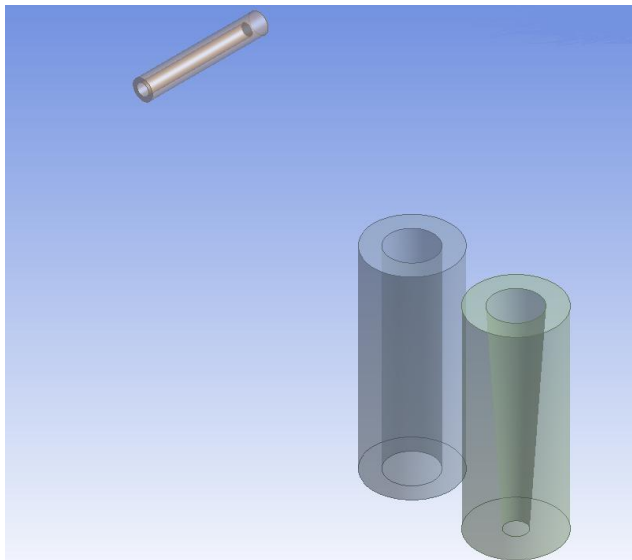


Figure 16: Final design of the clay bodies inside the oven.

The furnace itself has been designed as a simple cube in 108 147 150 which the right wall defined as inlet and the left wall as outlet. Three cylinders in different sizes are chosen as heat sinks placed inside the oven with different distances to the furnace's walls. There is a conflict between keeping down the computer cost, to increase the accuracy level and avoiding too many simplifications. Therefore geometry has been modeled with just three bodies. There is no regulation in terms of placing the ceramic bodies inside the oven in reality and that is the reason that two of the bodies have been modeled vertically on the bottom of the furnace with a little

distance between them. The third one has been placed horizontally somewhere further from inlet and the other bodies. The bodies are also in different sizes. The two standing ones are in 20×50 . The difference between them is at the bottom when one has a smaller open area at the bottom compared to the open area in the top of the body while the other one's open area at the top and bottom of the clay body has the same size. The third body is completely closed at the bottom and it is 5×30 . The bodies inside the oven are designed as porous bodies with a porosity of 0.5.

4.3.2 Mesh

Different meshes are created for the surface and inside the bodies. A simple sizing has been used for the surface of the oven and the surface of the bodies. For the inside part and also the wall regions, inflation is chosen for meshing. This is done to avoid mesh adaption further in FLUENT in y^+ adaption. Since the focus on present thesis is on water evaporation from the surfaces, the wall regions require accurate mesh. But in y^+ adaption each computational cell will be divided into 8 cells because division occurs in both horizontal and vertical directions. In inflation the amount of computational cells will be less and therefore less time and money would be needed for quite the same accuracy. Figures 17 and 18 show the mesh used during the simulations.

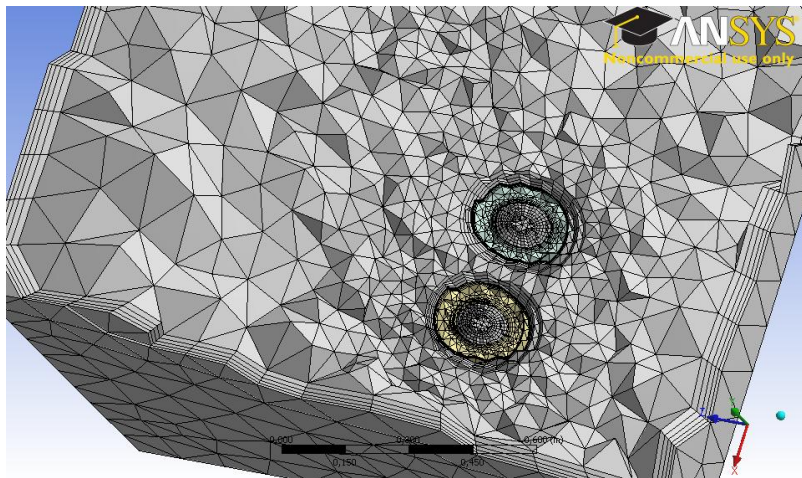


Figure 17: Overview of the mesh used during the simulations.

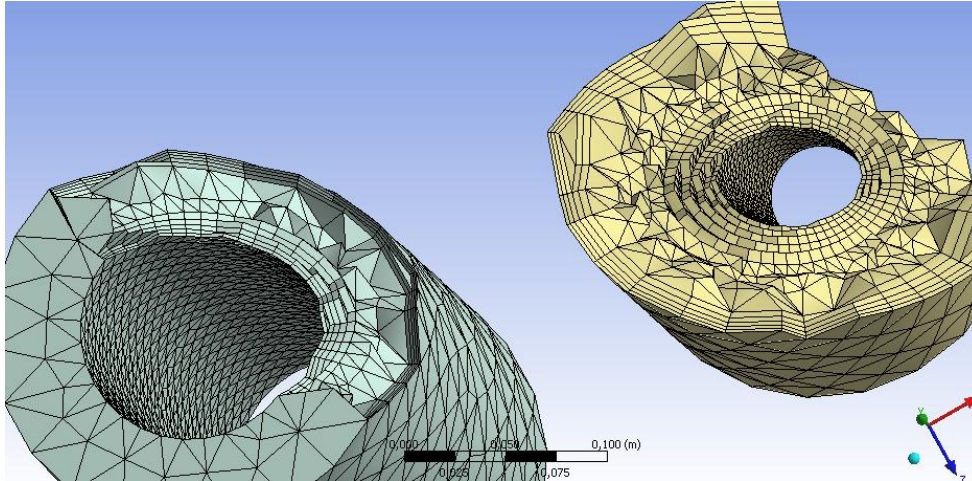


Figure 18: Close view of the clay bodies mesh during the simulations.

In figures 17 and 18, the tetra hedra shape of the cells can be simply identified. The number of cells is 103274 nodes with maximum skewness close to 0.90 element metrics.

4.3.3 Setting in FLUENT and Assumption

Since there is natural convection, the pressure variation is supposed to be small. The ideal gas law is used to estimate the relation between density and temperature. The flue gas is approximated to be air. One phase system in type of pressure based is solved. The pressure velocity coupling is solved with SIMPLE. When scheme with higher accuracy is used it is difficult to reach convergence. Convergence criteria that are used are scaled with residuals below 10^{-5} for all factors to increase number of iterations per time step and receive higher level of accuracy.

4.3.4 Boundary Condition

Pressure inlet is specified as the inlet condition and also temperature inlet from the collected data in the experiments in Indonesia. As it mentioned in chapter X the data given into the CFD simulations are from the experiments with only firewood as the fuel. Air and H₂O are chosen in material as fluid and dolomite is chosen as solid. For the outlet and operating conditions the pressure outlet is set. The gravity is defined to show the direction of the flow movement from inlet towards outlet. The $k-\omega$ turbulence model is recommended to solve the turbulence. It is a right solver in regions with low turbulence and low velocities. An advantage compared to other turbulence models is that there is no need of wall functions [5]. The $k-\omega$ model requires good grid resolution which is fulfilled according to boundary layers and size functions in areas by interest.

When the flow is low turbulent there must be at least one spot where the y^+ value is below five and a few spots with y^+ value below ten. This requirement is fulfilled. The y^+ values are low over the whole geometry.

4.3.5 Develop a Method for Evaporation and Langmuir Isotherm

The largest part of the added energy to the furnace will be consumed for vaporizing the water from the porous bodies inside the oven. A method for evaporation of water in the clay bodies has been developed. The evaporation is modeled as equilibrium chemical reactions (4.12). The evaporation is modeled as surface reactions on bodies. These are specified in FLUENT as fluids with a porosity of 0.5. The free water is initialized in the body and during the simulation the water is transported to the surfaces where the vaporization is occurred and then diffused with the flow.

$$(4.12)$$

To be able to develop the evaporation model, Langmuir's model [2] is used since it has many applications in surface kinetics. It is a semi-empirical isotherm derived from simple mass-action kinetics. Calling equation (4.12), the direct and inverse rate constants are k_1 and k_{-1} . If θ is defined as the fraction of the surface covered by adsorbed molecules, $1 - \theta$ is the fraction of the bare surface. The net rate of desorption is the difference between the rates of adsorption on the bare surface and desorption on the covered surface:

Where P is the partial pressure of the gas or in this case the molar concentration of water

At equilibrium k_1 and k_{-1} are very large i.e. $k_1 P \gg k_{-1} \theta$ and equation (4.13) reduces to

$$\theta = \frac{k_1 P}{k_1 P + k_{-1}}$$

Or

$$\theta = \frac{K P}{1 + K P}$$

Where K is adsorption- equilibrium constant and

$$K = \frac{k_1}{k_{-1}}$$

Due to the large temperature gradient the evaporation occurs very quickly and to be able to model the reactions in FLUENT it is needed to make them slower but at the same very close to the equilibrium in order to that both reactions i.e. adsorption and desorption keep up with each other. But the water in porous bodies dries very fast and it makes the FLUENT to calculate the reactions with some errors. That is the reason the value of Δt must be correct.

In FLUENT a converged steady state case with a developed flow field with inlet at 245°C is used as boundary condition. Then the reactions, increasing the temperature and transient property are introduced by the time we put water inside the bodies. The reactions are introduced in the model panel. The properties of the reactions are defined in the species transport panel. Site material in the porous body is defined as site 1 —as surface density and zero as molecule weight while the adsorbed water on these sites has been defined as water liquid with the right enthalpy and molecule weight. The total porous surface is defined as surface to volume ratio in the cell zone condition panel and is set to 139 —.

The activation energy and frequency factor are calculated for Arrhenius reactions in the model, however the activation energy for adsorption reaction is zero due to that the gas molecules don't need energy to condense and back to the water surface. The pre-exponential factor is varied to 10 times bigger in order to get the reaction works in FLUENT and in result get the water vaporized.

4.3.6 Assumption in Evaporation Model

Figure 19 shows the water trapped inside a pore. As it seen there are some computational cells between and . To model the evaporation from surface is assumed to be proportional to but it is more correct to be relating to or a value close to this. Using is numeric quickly but the problem is that it makes the evaporation rate very large. The model is also based on some other assumption such as the surface of the pores of the absorbent is homogeneous and adsorbed molecules do not interact.

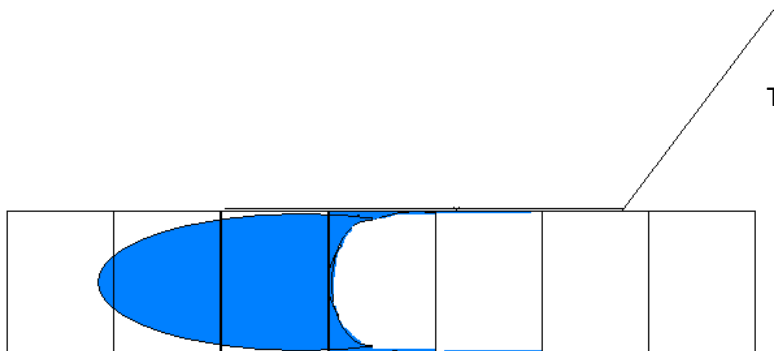


Figure 19: The water trapped inside the pore and the computational cells.

4.3.7 Bound Water and Evaporation

This model has been tried further with bound water. In this case 4 reactions are defined in FLUENT and two sites; one for free water and the other one for the combined water. Density of this water is set as 0.1 — i.e. the bound water is initially 0.1 of the free water. Notice that is just an assumption and for more correct value it is needed to weight the body continuously during the burning process. This amount is not completely accurate. The best is to weight a clay body during the burning process from time to time. It can be easily done in the lab in a small

oven. The bound water needs more energy to be vaporized. The required enthalpy is calculated and set as property of this water in material panel.

4.3.8 Radiation Model

Despite conduction and convection, in radiation the amount of heat transfer depends on both the temperature difference between two bodies and temperature level. In the studied case the highest experienced temperature is about 700°C. At this temperature there is no radiation from the gas flow inside the oven but between the clay bodies and the walls inside the oven the radiant-energy is exchanged. To model radiation in FLUENT a UDF is written and DO- model is used. As stated in chapter 3.4.7 an absorption coefficient has been defined in order to vary the bodies which reflect the heat from the ones which absorb it. In UDF the clay bodies have a large absorption coefficient while this amount for the rest is zero. For the walls in boundary condition the amount of heat flux is set as zero— and emissivity is set as 1.

5. Result and Discussion

The same as the method chapter, this chapter is also presented both the result from the experiments in Indonesia and the result from CFD simulations.

5.1 Experimental Results

The study cases are experimented in Pundong; one with firewood and coal briquette and the other one with only firewood as the fed fuel.

5.1.1 First Experience (Coal & Wood)

As mentioned in chapter 2.1, the first experience is done with combination of wood and coal briquettes due to be able to find another fuel for the traditional furnaces as the firewood's availability has been decreasing and its price has been increasing during years. The used coal briquettes have very low calorie and it is difficult to work with them. It takes long time they get burnt and it is not easy to cool off the fire at the end. The measurement of temperature has been continued until about one hour after burning. After that the oven should be left until it is cold enough to get the bodies out. The next morning, bodies have been taken out while 50% of the bodies are broken or cracked. Figure 20 shows the clay bodies after burning process.



Figure 20: The clay bodies after burning process.

As seen in figure 20, big cracks are found on the most of pottery bodies and also black spots on the surface of some of the bodies can be observed. After the bodies have been studied closer, it is seen that the black spots are only on the surfaces and not inside the mass. It proves that there is no reaction inside the clay which causes this color but it might be due to unburned carbon deposit. Since the temperature differences inside the furnace can cause shrinkage in the clay bodies, as shows in figure 21, a comparison between the temperatures of entered heat flow from two sides is done.

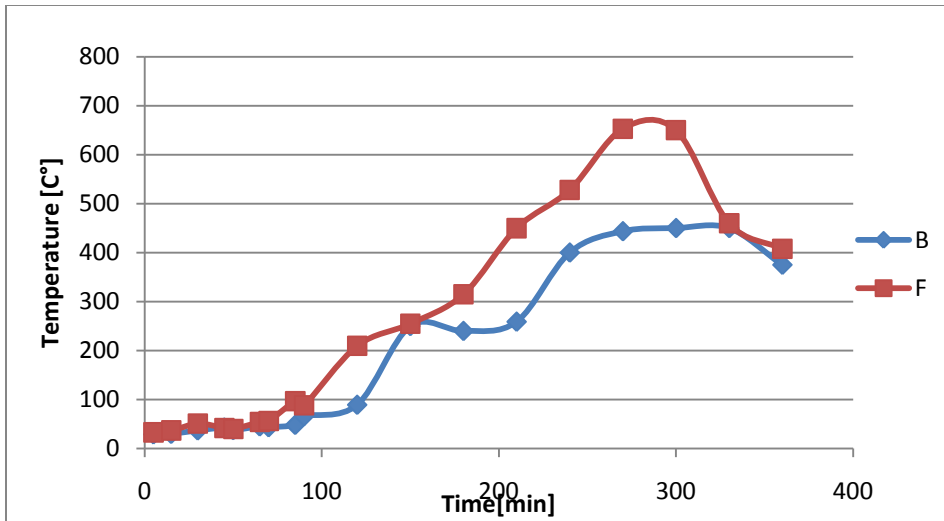


Figure 21: Comparison between the temperatures of entering heat flow from the two openings in the first experience.

The graphs in figure 21 indicate enormous difference between the temperatures of the heat flows. The heterogeneous temperature distribution will cause shrinkage in the body. To control the temperature differences inside the oven, a comparison between the temperatures close to the walls and in the middle of the kiln, where the bodies are placed on each other, is done as observed in figure 22.

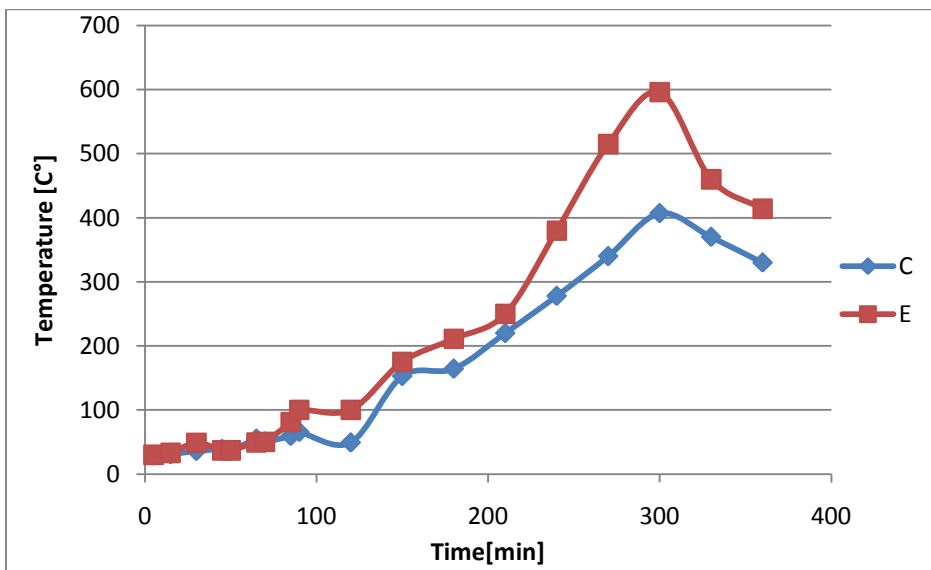


Figure 22: Comparison of the temperatures close to the wall and in the middle of the oven.

Figure 22 also proves a remarkable temperature difference in different places inside the oven which is the cause of cracks on the bodies.

5.1.2 Second Experience (Firewood)

The second burning experience has been run in the same place and in the same kiln as in the previous. In this experience no coal briquette has been used in the fuel. The decision has been made due to weak result from the earlier burning. Approximately the same result has been received from the second case. Figure 23 shows the ceramic bodies after burning.



Figure 23: The ceramic bodies after burning process.

As can be seen in figure 23, the chinks on the bodies are still available. Bigger cracks on the bottom might happen by static loading but the smaller ones would be the result of quick heating rate and incompletely dried green bodies. The bigger the pottery bodies are, the longer period is needed for them to be left outside before burning process. In this case, the bodies have been outside for only three days. Black spots are again found on the surface of some bodies due to unburned carbon deposit. A better convection might help the burning process. Figure 24 shows a comparison of the temperatures of entered heat flow from two sides of the kiln.

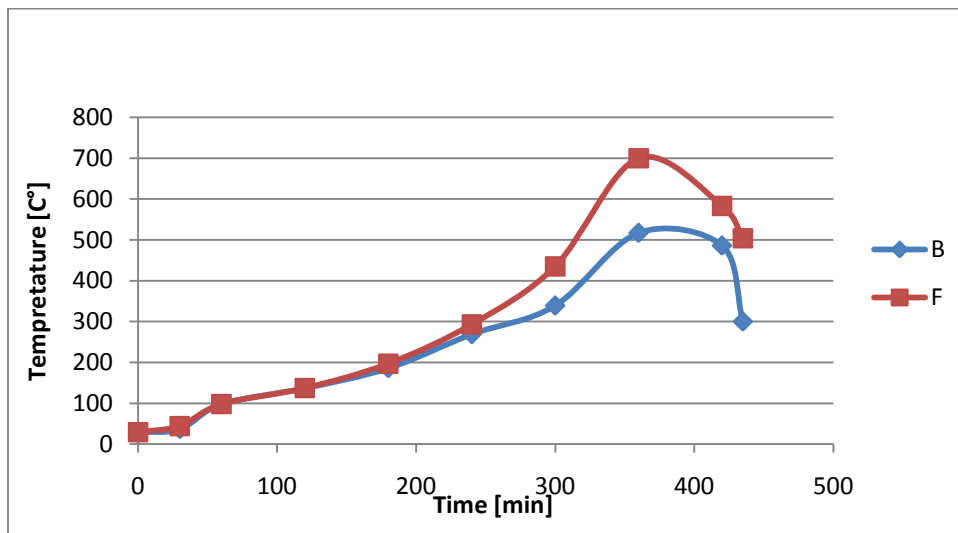


Figure 24: Comparison between the temperatures of entering heat flow from the two openings in the second experience.

As it observed in figure 24, uneven temperature distribution exists in the furnace. But because the fuel feeding is improved in this case the distribution of temperatures is less heterogeneous. In this experiment, the temperature of flame is also controlled and the result is shown in figure 25.

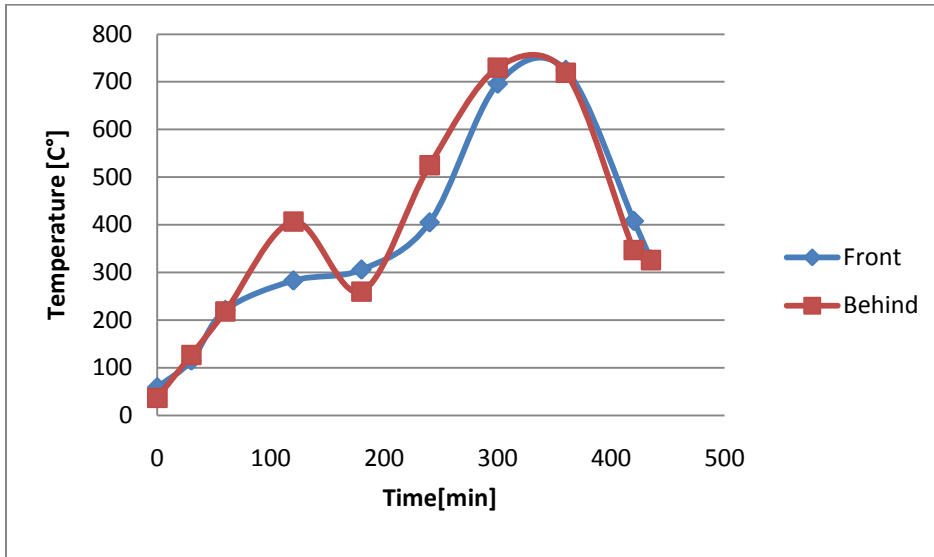


Figure 25: Comparison of the temperatures of flames.

Figure 25 proves a fair control over the fires in both sides of the furnace particularly at the end of the burning process. However, the results from the temperature measurements of front and back side of the kiln show a notable difference as seen in figures 26 and 27.

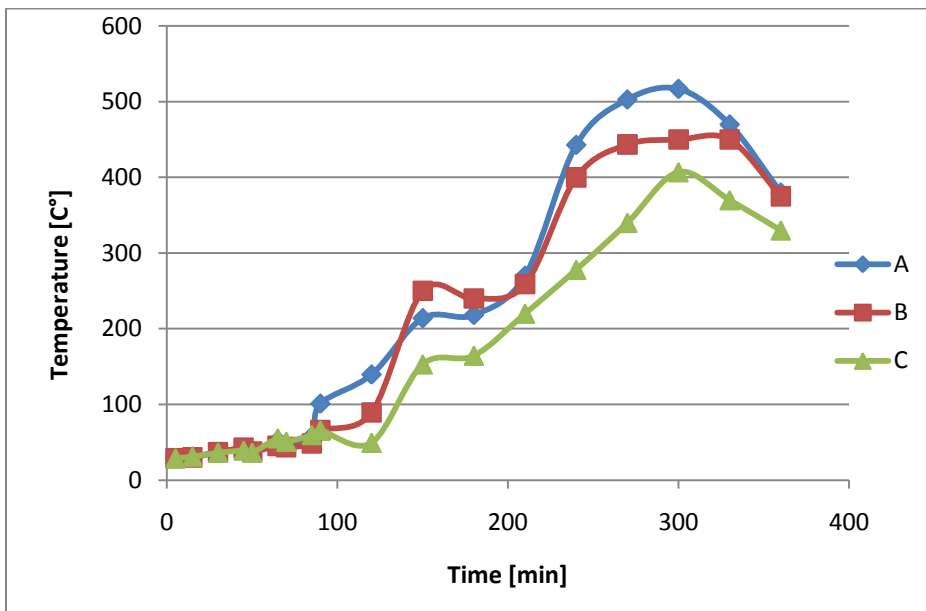


Figure 26: Temperatures measured from the front side.

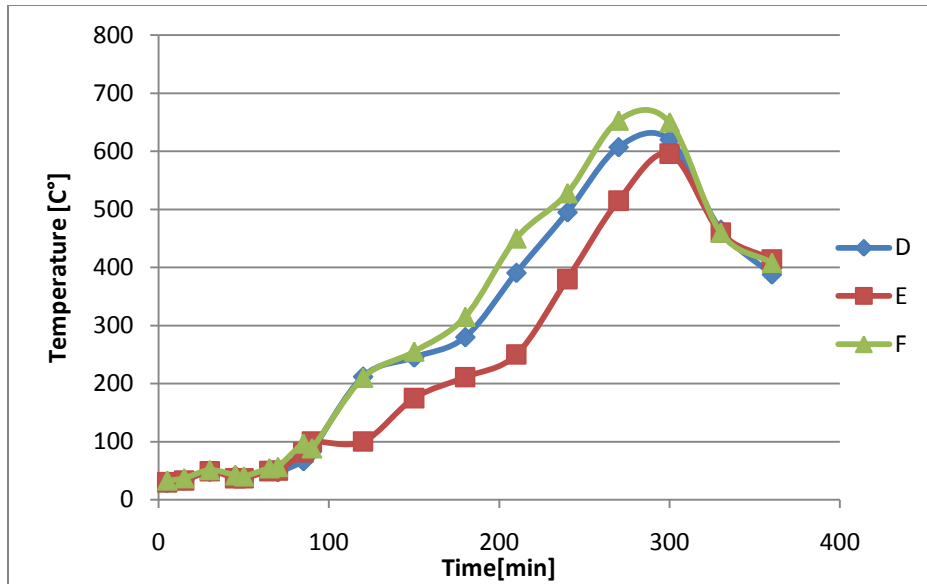


Figure 27: Temperatures measured from the back side.

As indicated in figures 26 and 27, the temperatures measured in the front side of the oven have not reached 600°C while the temperatures in the back side of the kiln have exceeded that temperature. This can happen due to the irregular packing of the clay bodies inside the oven or error in the measurements. It is hard to say that the measured data in a specific point shows the temperature of the gas flow there while there is a huge radiation from the walls inside the furnace which influence the thermometer. It is preferred to protect the thermometer from the radiative heat.

5.2 Discussion of the Experimental Results

In general, the wood used in the experiments has been from the wet season and it has had large water content. The temperature measurements from the outside of the furnace's walls show that the walls are not well isolated and have a lot of heat losses (See appendix D). The important heat losses are at the top of the furnace and also from the heat carrying by exhaust gasses. Large part of the fed energy loss is from radiative heat from the fire placements where the fire has high temperature. A cover which prevents the heat loss but allow the air to pass would be desirable. A total furnace efficiency of 14.2% for the experiment with coal and wood and 17.76% for the experiment with only wood are estimated (See appendix D). The efficiency of the furnace is low according to all described heat losses. The result is not completely correct due to the calculation is based on assumptions. Also the energy spent on loss of combined water is not included in the heat calculations. Radiation is also excluded the calculation however if the thermometer reaches a body surface or a wall inside the oven that temperature can be used in radiation calculation. In fact no complicated method is needed to measure the surface temperatures because there is a large temperature gradient between the gas flow and the clay body, and the thermometer has a very great thermal conductivity compare to both the flow gas and the clay.

5.3 CFD Results

At the beginning of the process, the temperature of 27°C is patched to the bodies inside the oven. The temperature is increased continuously during the process. The range of examined temperatures for modeling water evaporation is between 245- 699°C. Temperature contours show a little evaporation on the bodies' surfaces at the beginning but while the temperature increases, more amount of water is vaporized. Figure 28 shows the temperature contour at the middle of the two standing bodies.

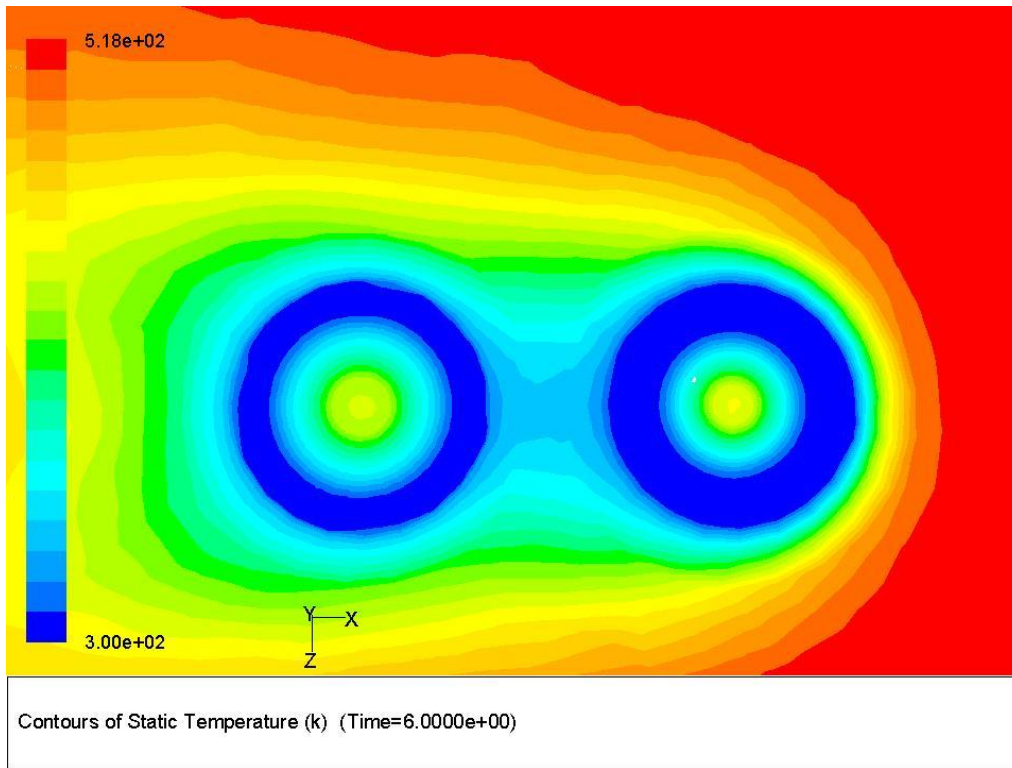


Figure 28: Temperature contour of the bodies at 518°C as the inlet temperature.

As shown in figure 28 the clay bodies and the spaces around them are colder than the other parts of the oven. The bodies are standing very close to each other but there is however a good distance between them. The space between the bodies has low temperature ($T= 343^{\circ}\text{C}$) and that is because the heat flow cannot reach that space effortlessly. Figure 29 shows a contour of static temperature when the inlet flow has reached its highest temperature ($T= 699^{\circ}\text{C}$).

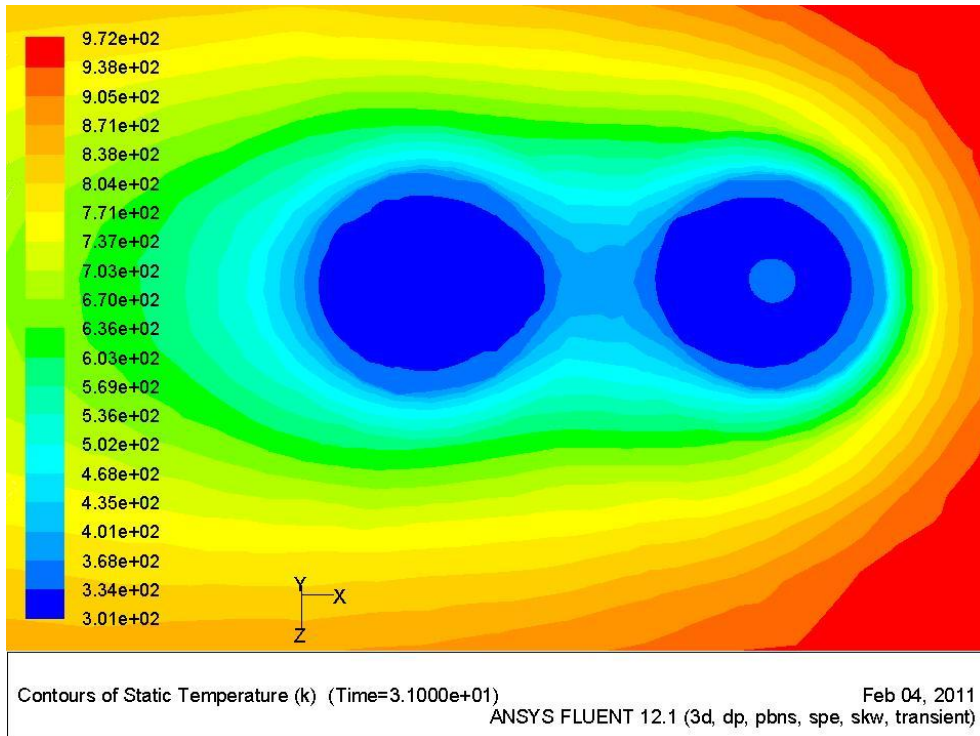


Figure 29: Temperature contour of the bodies at 699°C as the inlet temperature

As figure 29 indicates, at this temperature larger amount of the water has been vaporized and a temperature of 401°C has been reached between of the bodies.

In the next step, as it is stated in 4.3.7, the chemically bound water is introduced to the model. Figures 30 and 31 illustrate the contour of site surfaces of free water and the combined water respectively. It shows perfectly the water evaporation at 356°C after 6.5 seconds.

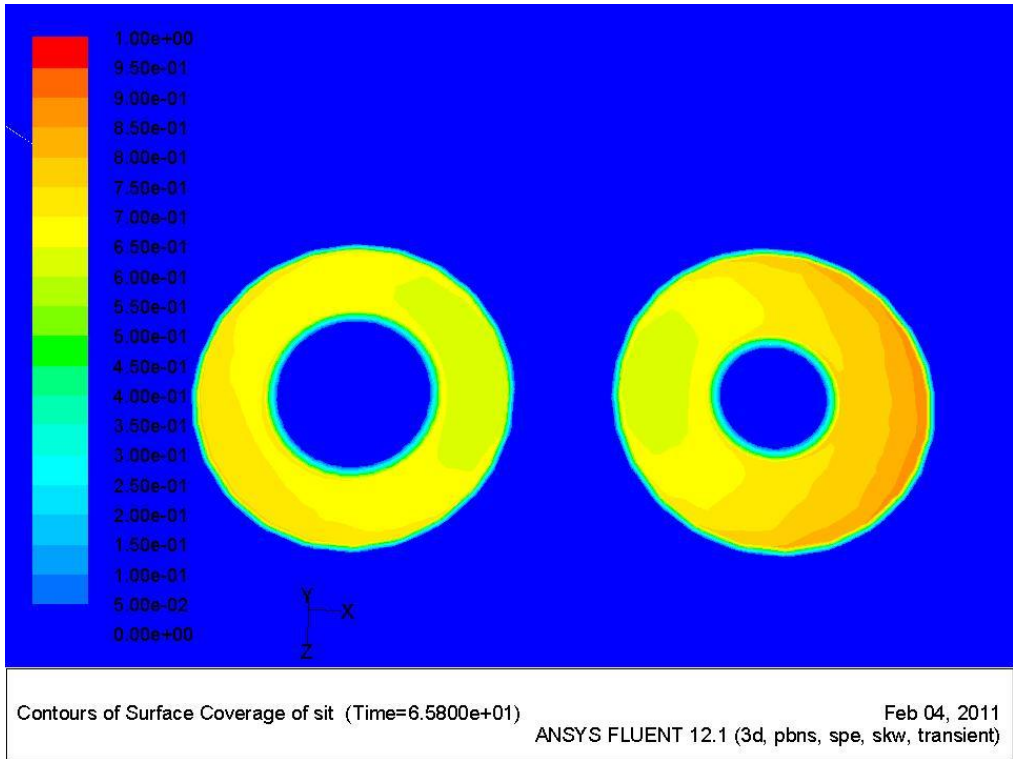


Figure30: The contour of dried surfaces from the free water.

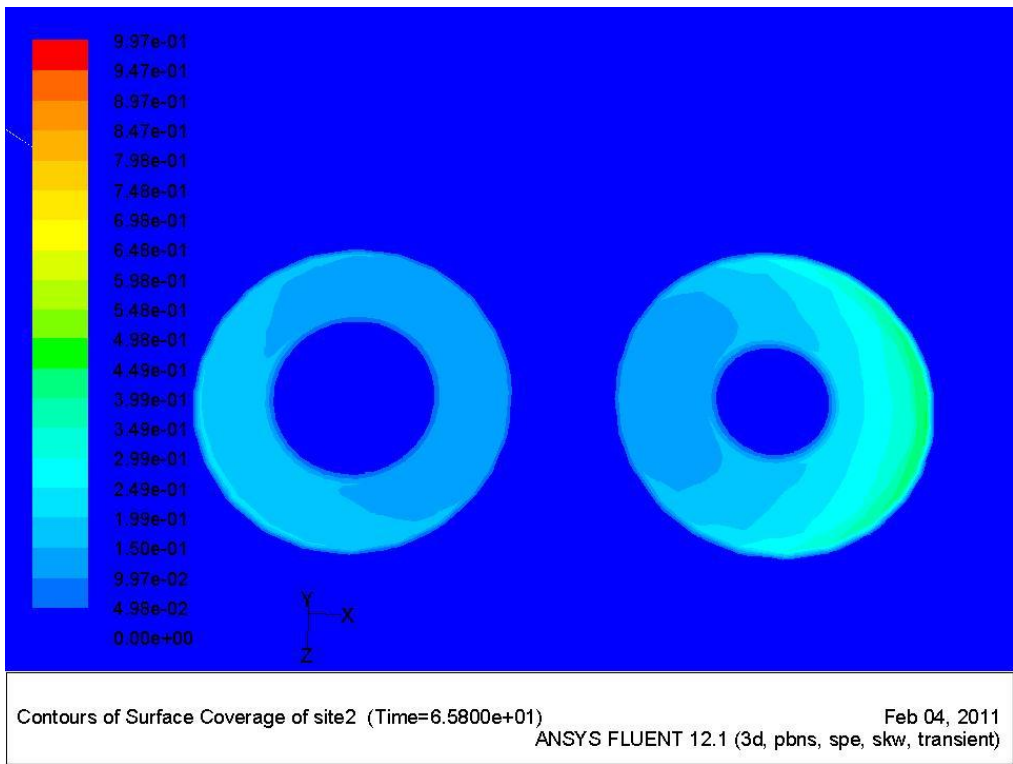


Figure 31: The contour of dried surface from the combined water.

Figure 31 proves how the evaporation model works successfully for the bound water the same as free water. It also verifies the theory in which says that the loss of combined water occurs around 400°C.

CFD simulation continues with adding a model for the effect of radiation. Figure 32 shows contour of static temperature at $T = 699^{\circ}\text{C}$ with the modeled radiation in the system.

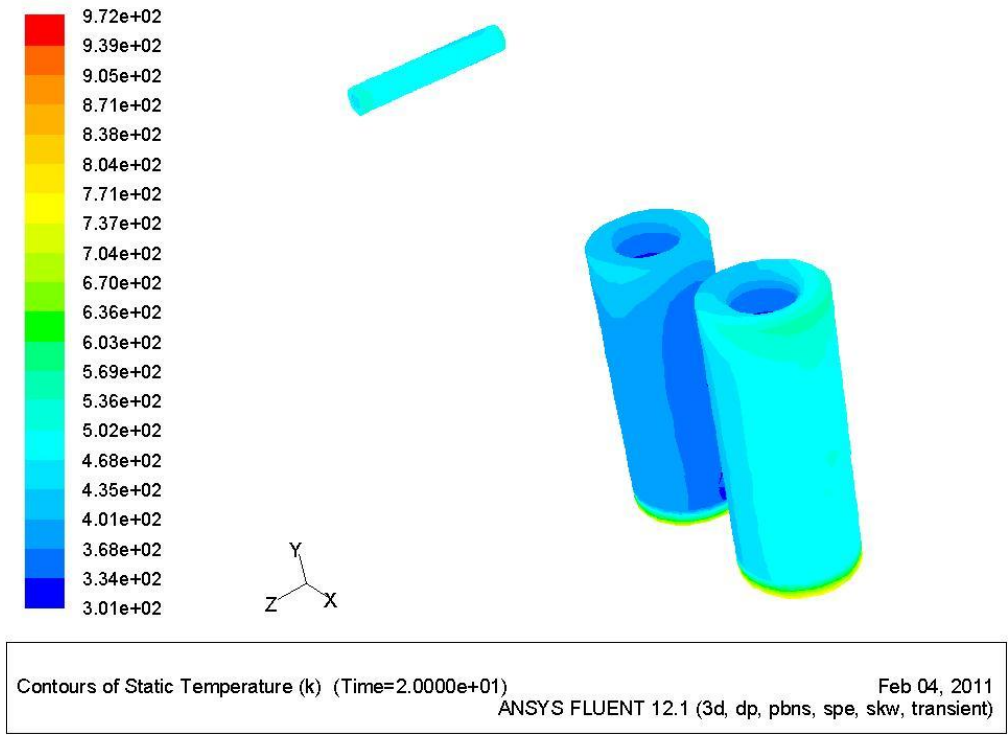
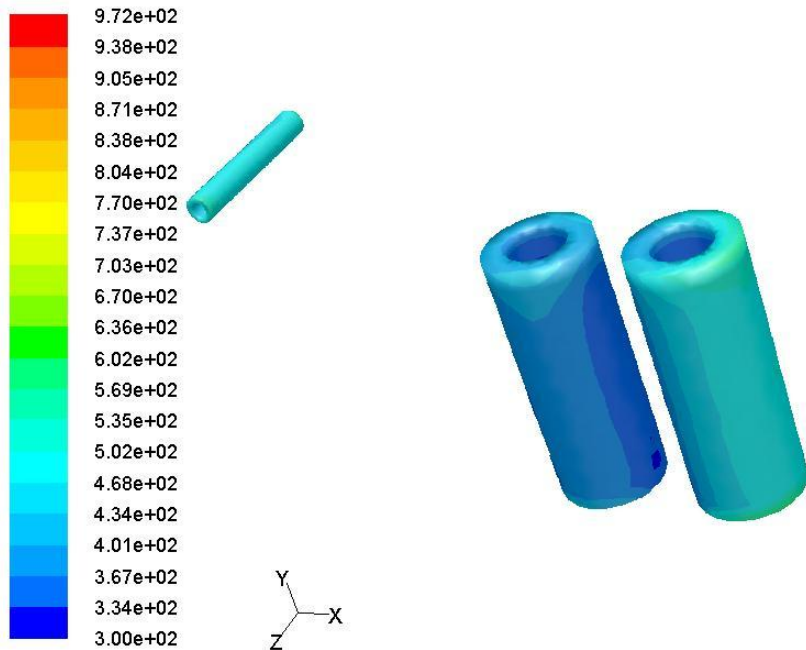


Figure 32: Contour of static temperature in the system with modeled radiation.

The highest temperature after 2 seconds running is $T = 737^{\circ}\text{C}$ which is seen at the bottom of the bodies. It can depend on the radiation rate from the bottom of the oven to the bodies. The temperature between the bodies is $T = 438^{\circ}\text{C}$. A comparison of this contour and the one without radiation gives remarkable results. As it is observed in figure 33 the highest achieved temperature is again at the bottom of the standing clay bodies. But the temperature is $T = 602^{\circ}\text{C}$.



Contours of Static Temperature (k) (Time=2.0000e+01)

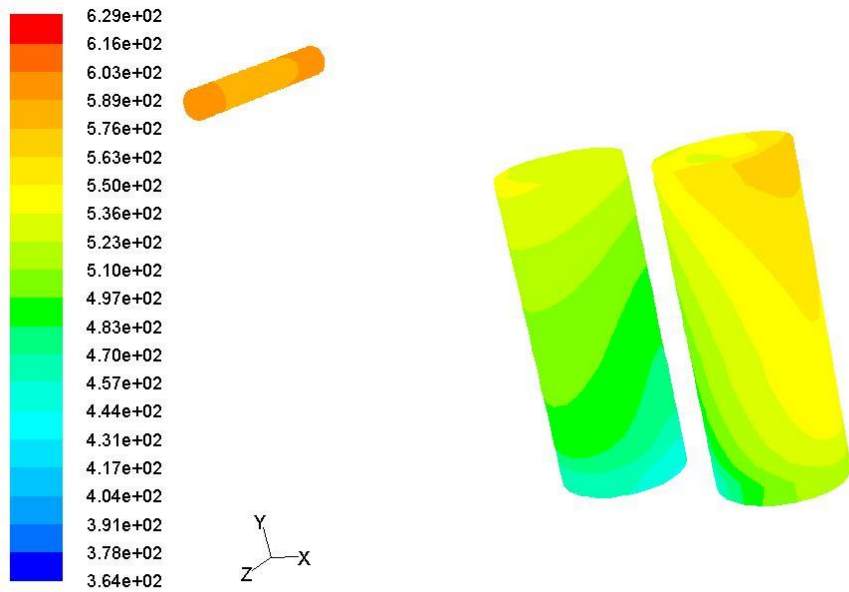
Feb 04, 2011

ANSYS FLUENT 12.1 (3d, dp, pbns, spe, skw, transient)

Figure 33: The contour of static temperature without radiation in the system.

Temperature contour in figure 33 indicates the temperature at $T = 401^{\circ}\text{C}$ between the two bodies which is less than the case with radiation. The effect of radiation on burning process is enormous specifically in the cases the clay bodies are placed close to each other. The reason is that the heat transfer via conduction is difficult in the spaces the flue gas cannot pass through. The problem is that in the lower temperature which the effect of radiation is weak, the bodies which are densely packed would not be able to get warmed completely.

As mentioned in 4.3.1 there is no regulation in terms of placing the ceramic bodies inside the oven and that is the reason that two of the bodies are modeled vertically on the bottom of the furnace with different geometries and a little distance between them. The third one which is smaller than the others is placed horizontally somewhere further from the inlet and the other bodies. Figure 34 shows how the geometry of the bodies and their location inside the oven affect the heat distribution.



Contours of Static Temperature (k) (Time=6.5800e+01) Feb 04, 2011
 ANSYS FLUENT 12.1 (3d, pbns, spe, skw, transient)

Figure 34: Heat distribution inside the oven.

As observed in figure 34, between the two bigger cylinders, the outer surface of the one closer to the inlet is warmer than the other bodies' surface. The little horizontal cylinder is almost dried. There are some reasons that can explain the reason that the smaller one is warmer. It can be due to the direction it is placed in the oven. It can depend on that the bottom of this body is closed, or it is simply because it is the smallest one. It should be mentioned that the contour plot is from the case with free and bound water and the radiation is not modeled.

For further studies of the effect of placing in heat transport inside the bodies, a velocity vector is used. As figure 35 shows when the bodies are placed vertically the heat flow never goes through the bodies. Considering that the whole at the bottom of the bodies is blocked by placing the bodies on the bottom it is seen that the velocity inside the bodies are zero and just some little swirls are observed in the beginning of the top side of the bodies.

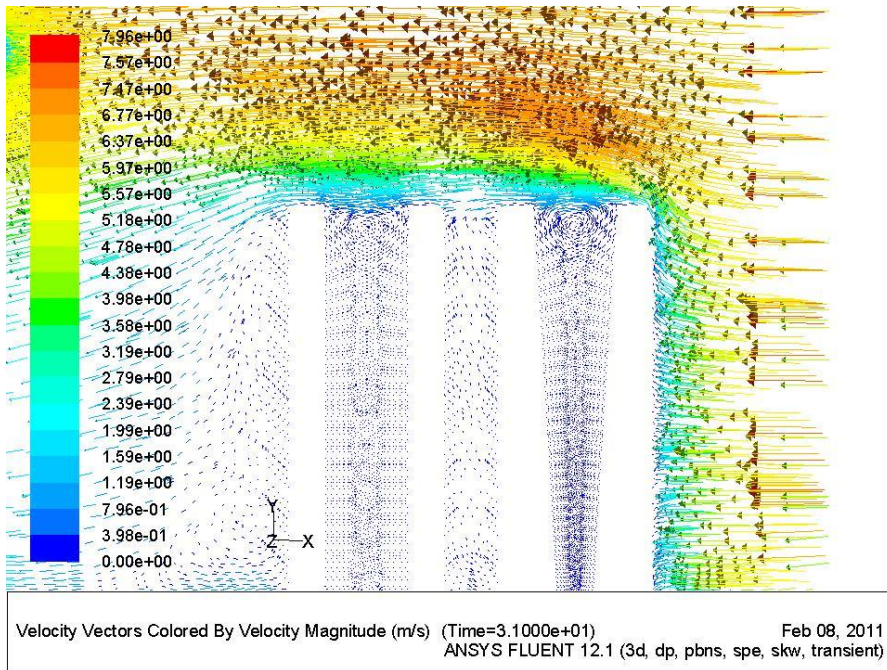


Figure 35: Velocity Vector of two standing bodies inside the oven.

As seen in figure 35 while the outer walls are drying the water is still remained inside the bodies and this is one the most important reasons of the crack on the pottery bodies.

Figure 36 is a density contour over the bodies and it shows how the air inside the bodies is heavier than the air above them.

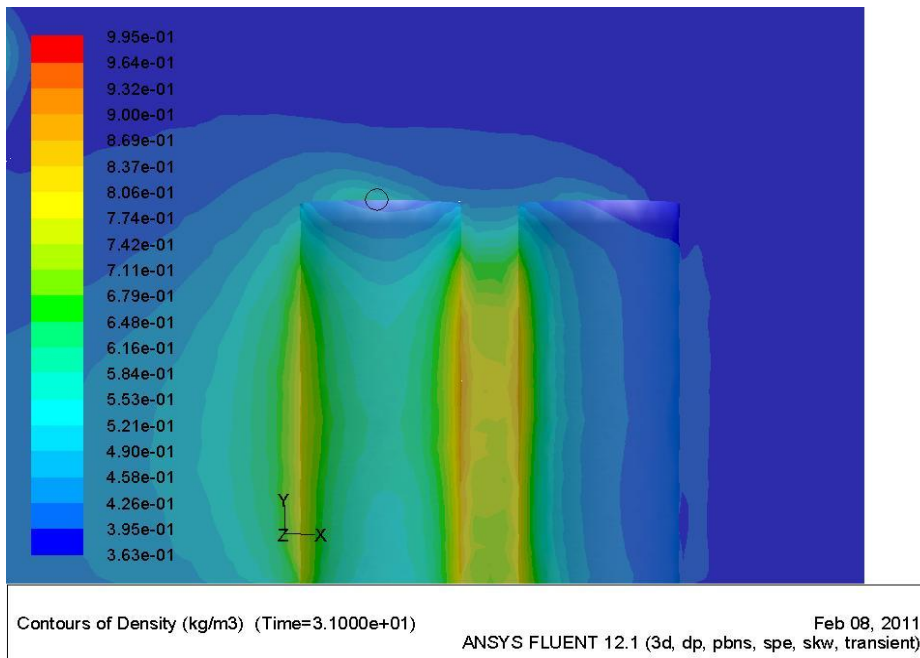


Figure 36: The contours of density over the standing ceramic bodies

As it is observed in figure 36 the air inside the bodies is colder and heavier and it cannot go up. It gets stuck inside the body and there is no air circulation through the bodies.

5.4 Discussion of the CFD Results

In the modeling with $k-\omega$ the turbulent length scale is not determined. It can be estimated by the hydraulic diameter. Since the inlet condition is unknown it is preferable to read k value from developed flow profile at a distance from inlet and use that value in boundary conditions. In order to model the conduction the bottom of the kiln should be defined with specific boundary conditions. However conductive heat transfer from the bottom of the oven through inside is not modeled in the present CFD simulations due to technical restrictions.

To avoid the surface stiff solution, a small time scale is chosen for the simulations. There is a struggle between keeping down the computer cost and increase the accuracy level. It has been tried to choose an acceptable time scale for simulations to keep the computational time low but during all the simulations the warning of stiff solver is observed.

The result from the simulation with bound water shows contradiction with reality since the water is vaporized at about 40°C instead of 100°C. The reason might be invalid assumption during calculations of the rate reactions.

6. Conclusions

Decomposition of clay to amorphous silica and alumina requires a temperature of 900°C which is the ideal temperature in traditional pottery industry. The obtained maximum temperature is sufficient enough to remove the free water and the chemically bounded water and the result from water evaporation model in CFD approve this. The temperature varies significantly in the furnace and this impact the quality of the clay bodies due to risk of cracks. The packing of the clay bodies in the furnace also affect the risk of cracks due to when bodies are placed compactly the effect of radiation in heat transfer will be eliminated. The efficiency of the furnace is low due to heat losses on the top and from the channels under the furnace. It is possible to simulate the burning process in the furnace with carefully prepared assumptions. CFD is a powerful tool to model the burning process. Evaporation model can also be simulated however there are some problems due to fast rate of reactions but with better assumptions and more accurate calculations the result would be even more trustworthy.

7. Future Work

In practical works:

The most important issue in this project is to access accurate temperature data. Further measurements would provide more accurate results. By protecting the thermometer from heat radiation inside the oven, more accurate temperature of the gas flow would be obtained. The measurement of the clay bodies can provide required data to calculate radiation. Therefore radiation can be easily included in heat calculation. Precise way of measuring the body's weight after burning is very important because the amount of water simulated in CFD is based on the water loss measured experimentally. Amount of combined water in a clay body be also measured continuously during an experimental burning process in the laboratory. An analysis of the flue gas composition would be of interest. It would be possible to measure the CO₂ content which would explain the exact air intake to the furnace. The mineral composition of the clay, wood and briquette must be inspected in the laboratory due to prevent any unnecessary assumption. The moisture content in the fuel and the clay bodies before burning can be measured in laboratory.

In CFD simulations:

The better assumption and correct calculation during the formation of the evaporation model s necessary. Better simulations which include conduction, convection and radiation would give a good overview on the process. The geometry should be improved with more sink subject inside the oven which can picture the real situation better.

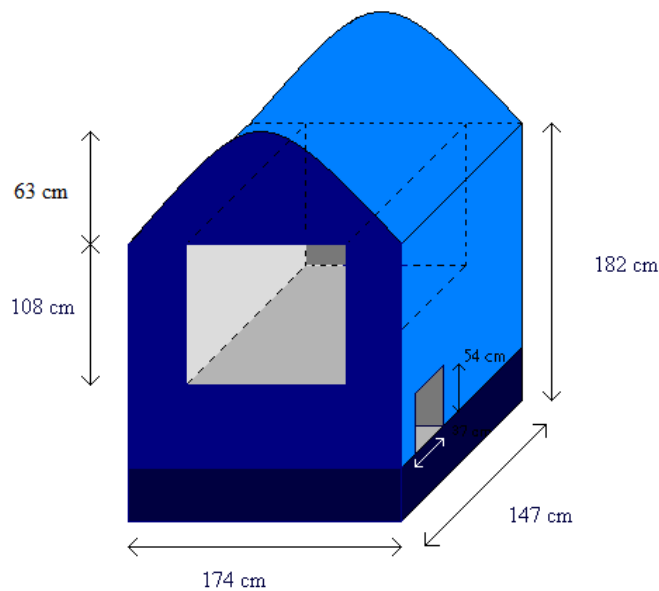
8. References

1. **W.G. Lawrence, R.R. West.** *Ceramic Science for the Potter*, 2nd edition. u.o. : Chilton book company, 1982.
2. **Seader J.D. and Henley E.J.** *Separation Process Principles*, 2nd edition, Wiley 2006.
3. **R. B. Keey.** *Drying of loose and particulate materials*, Hemisphere Publishing Corporation, 1992.
4. **James R. Wiley, Charles E. Wicks, Robert E. Wilson, Gregory Rorrer.** *Fundamentals of Momentum, Heat and Mass transfer*. u.o. : John Wiley & Sons, 2001, 4th edition.
5. **Bengt Andersson, Ronnie Andersson, Love Håkansson, Mikael Mortensen, Rahman Sudiyo, Berend van Wachem.** *Computational Fluid Dynamics for Chemical Engineers*. Gothenburg : u.n., 2008.
6. **FOGLER, H. SCOTT.** *Elements of Chemical Reaction Engineering*. u.o. : Pearson Education, 2006, 4th edition.
7. **Cecilia Schotte.** *CFD Simulation of Flue Gas Flow in Traditional Kasongan Pottery Furnace*: Chalmers University of Technology, Gothenburg, 2010.
8. **Sam E.H. Robjer Gullman.** *Development of evaporation models for CFD*: Chalmers University of Technology, Gothenburg, 2010.

Appendix A:

Dimension:

1. The tower (not shown in the figure below): the height: 295 cm, the width: 70 cm, the length: 75 cm
2. The distance between kiln and tower (not shown in the figure below): 121 cm
3. The dimension of the entrance of fire place: the width: 37 cm, the height: 54 cm
4. The dimension of kiln: the height of crown: 63 cm, the height of square part of kiln: 182 cm the width of kiln 174 cm, the length of kiln: 147 cm
5. The dimension from under the crown until the bottom of kiln: 108 cm
6. The thickness of wall around: 11.5 cm
7. The dimension of entrance of heat flow inside the kiln: the length: 39 cm, the width: 23 cm
8. The dimension of heat exhaust inside the kiln: the length: 174 cm, the width: 13 cm



- The black part is a plate the oven is built on it.

Appendix B:

The data resulting from the first burning (Wood & Briquette):

Table1: The data from weigh measurement of clay body before and after burning.

Model	Amount		weight [kg]						Total
			Before		After		Difference		
1		6	3.7	22.2	2.6	15.6	1.1	6.6	
2		6	3.6	21.6	2.2	13.2	1.4	8.4	
3		6	6.2	37.2	4.5	27	1.7	10.2	
4		4	3	12	2.3	9.2	0.7	2.8	
5		6	5.6	33.6	4.2	25.2	1.4	8.4	
6		12	4	48	3	36	1	12	
7		6	3.5	21	2.8	16.8	0.7	4.2	
8		6	3.8	22.8	2.6	15.6	1.2	7.2	
9		5	7.5	37.5	5.4	27	2.1	10.5	
10		6	2.5	15	1.1	6.6	1.4	8.4	
11		3	4.9	14.7	3.8	11.4	1.1	3.3	
12		3	4.5	13.5	3.6	10.8	0.9	2.7	
13		2	1	2	0.9	1.8	0.1	0.2	
14		4	4.8	19.2	3.9	15.6	0.9	3.6	
15		2	3.2	6.4	2.4	4.8	0.8	1.6	
16		2	3.8	7.6	2.8	5.6	1	2	
17		4	1.4	5.6	1	4	0.4	1.6	
18		4	6.2	24.8	4.9	19.6	1.3	5.2	
19		4	4.3	17.2	3.1	12.4	1.2	4.8	
20		4	3.6	14.4	2.6	10.4	1	4	
		95		396.3		288.6		107.7	

Table 2: The data extracted from temperature measurements

	point to measure the temperature					
time(min)	A	B	C	D	E	F
	the temperatures (C°)					
5	29	29	29	29	30	33
15	31	30	31	33	33	37
30	37.1	37	36.2	48	48.9	51
45	42	42.7	39.1	42	37	42
50	38.1	37.7	36.3	37.2	37	40.1
65	52	45.2	55.3	51.8	49.3	54.2
70	43.6	43.5	50.8	47.5	50.2	56.4
85	57.7	48.3	59.7	66.4	81.4	96.7
90	101	66	65.9	83.5	100.2	88.5
120	139.5	89.3	49.4	212	100.2	210
150	214	250	153	245	175	255
180	218.2	240	164.5	280	211.1	315
210	270	258.9	220	390.7	250	450
240	443	400	278	495	380	528
270	503	443.5	340	607.1	515	653
300	517	450	407	620	596	650
330	470	450	370	465	460	460
360	380	375	330	388	414	408

Table 3: The temperature data of exhaust gases.

temparatet of exhaustet gases		
	time[min]	temp [C°]
11:19	42	33
12:10	93	40.3
13:10	153	62
15:25	288	130
16:18	341	140
16:44	387	150
17:02	429	70

Appendix C:

The data resulting from the second burning (Wood):

Table1: The data from weigh measurement of clay body before and after burning

Model	Amount	weight [kg]						Total
		Before		After		Difference		
1	7	2.7	18.9	2.0	14.0	0.7	4.9	
2	9	0.8	7.2	0.3	2.7	0.5	4.5	
	6	1.3	7.8	0.9	5.4	0.4	2.4	
3	3	1.6	4.8	1.0	3.0	0.6	1.8	
	8	1.1	8.8	0.8	6.4	0.3	2.4	
4	20	1.2	24.0	0.8	16.0	0.4	8.0	
	20	1.0	20.0	0.6	12.0	0.4	8.0	
	20	0.8	16.0	0.3	6.0	0.5	10.0	
5	2	2.7	5.4	2.3	4.6	0.4	0.8	
6	6	3.0	18.0	2.5	15.0	0.5	3.0	
7	6	5.8	34.8	4.2	25.2	1.6	9.6	
8	1	3.9	3.9	3.1	3.1	0.8	0.8	
9	1	2.7	2.7	1.8	1.8	0.9	0.9	
10	3	4.1	12.3	3.2	9.6	0.9	2.7	
11	5	4.9	24.5	3.0	15.0	1.9	9.5	
12	5	4.9	24.5	3.9	19.5	1.0	5.0	
13	10	11.7	117.0	8.6	86.0	3.1	31.0	
14	6	3.7	22.2	2.6	15.6	1.1	6.6	
15	5	5.4	27.0	3.2	16.0	2.2	11.0	
16	5	3.3	16.5	2.7	13.5	0.6	3.0	
			416.3		290.4	125.9	125.9	

Table 2: The data extracted from temperature measurements

		Time (min)	0	30	60	120	180	240	300	360	420	435
Point												
Behind	A1	29	31	67	102	196	235	380	525	501	410	
	A2	29	39	100	135	177	223	328	480	510	317	
	A3	31	34	35	39	38	38	53	50	51	42	
	B1	29	32	95	128	518	629	676	972	791	652	
	B2	29	37	98	137	186	269	339	517	486	300	
	B3	31	35	36	38	38	40	50	43	51	45	
	C1	29	32	72	108	195	250	426	561	523	402	
	C2	29	38	88	105	158	191	318	406	487	353	
	C3	31	34	35	38	37	39	55	47	49	47	
Front	D1	29	37	66	132	208	315	397	571	491	408	
	D2	29	41	98	126	196	220	352	515	545	379	
	D3	31	34	37	44	42	66	82	100	105	59	
	E1	29	35	65	127	151	180	334	478	491	353	
	E2	29	40	86	134	161	182	346	490	536	308	
	E3	31	33	37	40	44	46	86	77	83	60	
	F1	29	38	120	142	494	688	783	1015	745	633	
	F2	29	44	98	137	197	293	435	700	583	504	
	F3	31	33	40	44	44	51	83	76	87	64	
Flame front	FR1	59	115	221	283	306	405	696	725	408	327	
out down	FR2	44	60	42	53	65	72	90	64	90	62	
out up	FR3	42	54	35	44	47	45	44	48	57	50	
Flame behind	BA1	37	127	218	407	260	525	730	719	347	326	
out down	BA2	35	50	50	66	63	68	85	110	74	61	
out up	BA3	35	48	40	49	47	44	52	53	59	51	

Table 3: The temperature data of exhaust gases.

time (min)	0	30	90	120	180	240	300	360	390	405
ex ©		36	40	50	332	340	365	399	410	411

Appendix D:

The result from the heat calculations

Q wood	517500	kcal	Q wood	666300	kcal
Q briquett	194000	kcal	Q briquett	0	kcal
Q 1	58158	kcal	Q 1	67986	kcal
Q 2	7646	kcal	Q 2	8938	kcal
Q 3	35844	kcal	Q 3	41411	kcal
Qinput	711500	kcal	Qinput	666300	kcal
Efficiency	14.2	%	Efficiency	17.76	%

vaporization water	Q1
sensible heat of water	Q2
sensible heat of clay	Q3